

# SCIENTIFIC REPORTS



OPEN

## Calcium and Magnesium Ions Are Membrane-Active against Stationary-Phase *Staphylococcus aureus* with High Specificity

Yuntao Xie<sup>1,2</sup> & Lihua Yang<sup>1,2,3</sup>

Received: 04 September 2015

Accepted: 06 January 2016

Published: 11 February 2016

*Staphylococcus aureus* (*S. aureus*) is notorious for its ability to acquire antibiotic-resistance, and antibiotic-resistant *S. aureus* has become a wide-spread cause of high mortality rate. Novel antimicrobials capable of eradicating *S. aureus* cells including antibiotic-resistant ones are thus highly desired. Membrane-active bactericides and species-specific antimicrobials are two promising sources of novel anti-infective agents for fighting against bacterial antibiotic-resistance. We herein show that  $\text{Ca}^{2+}$  and  $\text{Mg}^{2+}$ , two alkaline-earth-metal ions physiologically essential for diverse living organisms, both disrupt model *S. aureus* membranes and kill stationary-phase *S. aureus* cells, indicative of membrane-activity. In contrast to *S. aureus*, *Escherichia coli* and *Bacillus subtilis* exhibit unaffected survival after similar treatment with these two cations, indicative of species-specific activity against *S. aureus*. Moreover, neither  $\text{Ca}^{2+}$  nor  $\text{Mg}^{2+}$  lyses mouse red blood cells, indicative of hemo-compatibility. This work suggests that  $\text{Ca}^{2+}$  and  $\text{Mg}^{2+}$  may have implications in targeted eradication of *S. aureus* pathogen including the antibiotic-resistant ones.

*Staphylococcus aureus* (*S. aureus*) is a Gram-positive bacterium notorious for its ability to acquire antibiotic-resistance<sup>1</sup>. Antibiotic-resistant strains of *S. aureus* have emerged as a widespread cause of both hospital- and community-associated infections, leading to high mortality rate<sup>1–3</sup>. For example, methicillin-resistant *S. aureus* is estimated to cause >11,000 deaths per year in the United States<sup>4</sup>. It is thus imperative to discover/develop antimicrobials that are both active against *S. aureus* including antibiotic-resistant strains and less prone to evoke resistance.

Antimicrobial peptides (AMPs) are nature's antibiotics still in action despite of their evolutionarily ancient origins. Many AMPs act by impairing the barrier function of bacterial membranes<sup>5–11</sup>, a generic mode that appears to be more difficult for bacteria to circumvent than the metabolic-targeting modes of conventional antibiotics<sup>12</sup>. By capturing the structural features common to most AMPs (*i.e.*, being simultaneously cationic and amphiphilic), synthetic mimics of AMPs (SMAMPs) have demonstrated similar *in vitro* antibacterial activity and membrane-destabilizing modes as do AMPs<sup>13–42</sup>. Despite of the great potentials, AMPs and SMAMPs are effort- and, often, cost-consuming to produce, which has significantly hindered their pharmaceutical development. Alternative to AMPs and SMAMPs, species-specific antimicrobials have recently been proposed as a promising source of anti-infective agents that are less prone to evoke resistance<sup>43</sup>. Therefore, antimicrobials that are readily available and simultaneously membrane-active and species-specific against *S. aureus* are highly desired.

Metal ions are readily available, and certain transition-metal ions (*e.g.*,  $\text{Cu}^{2+}$ ,  $\text{Hg}^{2+}$ ,  $\text{Zn}^{2+}$ , and  $\text{Cd}^{2+}$ ) have demonstrated wide-spectrum antibacterial efficacy to varying extent<sup>44,45</sup>. A best known example might be  $\text{Ag}^{+}$  ion, which is active against both Gram-negative and -positive bacteria<sup>46,47</sup>. Nevertheless, use of heavy metal ions as disinfectants may adversely impact the host and/or the environment. Besides, the action modes by which these heavy metal ions achieve their antibacterial activity remain elusive. Having these concerns in mind, we hence turn to non-transition metal ions, in efforts to find candidates for specifically disrupting *S. aureus* membranes.

<sup>1</sup>CAS Key Laboratory of Soft Matter Chemistry, University of Science and Technology of China, Hefei, Anhui 230026 China. <sup>2</sup>Department of Materials Science and Engineering, University of Science and Technology of China, Hefei, Anhui 230026 China. <sup>3</sup>Department of Polymer Science and Engineering, University of Science and Technology of China, Hefei, Anhui 230026 China. Correspondence and requests for materials should be addressed to L.Y. (email: lhyang@ustc.edu.cn)

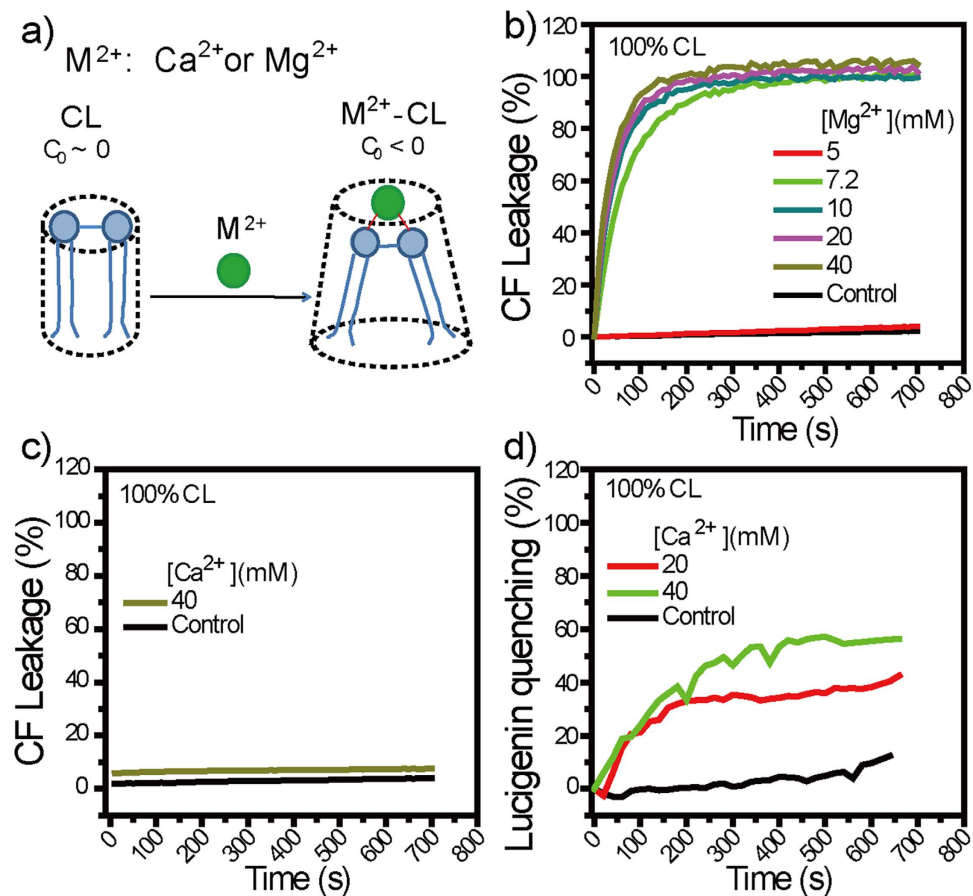


**Figure 1.** (a) Binding of  $M^{2+}$  ( $M = Ca, Mg$ ) with cardiolipin (CL), the major lipid component in *S. aureus*, converts the originally zero-intrinsic-curvature ( $C_0 \sim 0$ ) lipid into  $M^{2+}$ -CL complexes with negative intrinsic curvature ( $C_0 < 0$ ). (b–d) Dye leakage assays using large unilamellar vesicles (LUVs) composed of 100% CL as a first-order model for *S. aureus* membranes. (b)  $Mg^{2+}$  at  $\geq 7.2$  mM caused significant carboxyl fluorescein (CF) leakage. (c,d)  $Ca^{2+}$ , though (c) unable to cause detectable CF leakage, caused (d) appreciable quenching in the fluorescence intensity of intravesicular lucigenin. Controls are samples assayed similarly but without  $M^{2+}$  additions.

Calcium and magnesium ions ( $Ca^{2+}$  and  $Mg^{2+}$ ) are two alkaline-earth-metal ions ( $M^{2+}$ ) physiologically essential to almost all living organisms<sup>48</sup>. Upon binding with cardiolipin (CL), a major lipid component in *S. aureus* membranes<sup>49,50</sup>,  $M^{2+}$  ( $M = Ca, Mg$ ) forms  $M^{2+}$ -CL complexes of negative curvature (Fig. 1a)<sup>41,51</sup>, and negative curvature is a physical parameter necessary for a variety of membrane-destabilization processes as has been validated for those induced by AMPs and SMAMPs<sup>11,39–42</sup>. We therefore hypothesize that  $Ca^{2+}$  and  $Mg^{2+}$  may be membrane-active, species-specific agent against *S. aureus*. To test this hypothesis, we perform vesicle membrane permeabilization assays and antibacterial assays and find that, at  $\leq 40$  mM, both  $Ca^{2+}$  and  $Mg^{2+}$  disrupt model *S. aureus* membranes and kill stationary phase *S. aureus* cells, indicative of membrane-activity. In contrast to *S. aureus*, *Escherichia coli* and *Bacillus subtilis* exhibit unaffected survival after similar treatment with these two cations, indicative of species-specific activity against *S. aureus*. Moreover, within the tested dose range, neither  $Ca^{2+}$  nor  $Mg^{2+}$  is hemolytic against mouse red blood cells, indicative of good hemo-compatibility. Collectively, these results suggest that  $Ca^{2+}$  and  $Mg^{2+}$  may have implications in targeted eradication of *S. aureus* pathogen including antibiotic-resistant ones.

## Results and Discussion

$M^{2+}$  ( $M = Ca, Mg$ ) binds with CL to form  $M^{2+}$ -CL complexes of negative curvature (Fig. 1a)<sup>41,51</sup>, and negative curvature promote membrane destabilization as validated for cases with AMPs and SMAMPs<sup>11,39–42</sup>. We hence evaluated whether  $Ca^{2+}$  and  $Mg^{2+}$  destabilizes *S. aureus* membranes, using mono-component large unilamellar vesicles (LUVs) composed of CL as our first order model of *S. aureus* membranes and performing dye leakage assays<sup>39,41,52–57</sup>. To dissect the effect of  $M^{2+}$  dose from those of ionic strength and osmolarity, we use  $M^{2+}$ -supplemented HEPES buffers (Table 1) which have ionic strength and osmolarity kept almost constant but varying  $MCl_2$  concentration; these same buffers are used for all experiments throughout this work. The first dye probe we used is carboxyl fluorescein (CF), a membrane-impermeant molecule with a hydrodynamic diameter of  $\sim 1$  nm and negatively charges at physiological pH<sup>58–62</sup>.  $Mg^{2+}$ , once  $\geq 7.2$  mM, caused  $\sim 100\%$  CF leakage from CL LUVs (Fig. 1b), indicative of  $Mg^{2+}$ -induced CF efflux across CL membranes.  $Ca^{2+}$ , though unable to cause

M <sup>2+</sup> (mM)	HEPES (mM)	NaCl (mM)	Sucrose (mM)
0	10	170	0
5	10	155	0
10	10	140	15
20	10	110	45
40	10	50	105

**Table 1.** Mg<sup>2+</sup> and Ca<sup>2+</sup> doses in 10 mM HEPES buffer<sup>a</sup>. <sup>a</sup>HEPES, NaCl, and sucrose were supplemented to help keep the pH, final ionic strength and final osmolarity constant at 7.4, 170 mM, and 325–340 RT (where R is the gas constant and T is ambient temperature, and ideal solutions are assumed), respectively. Same buffers were used for all experiments through this work unless specified otherwise.

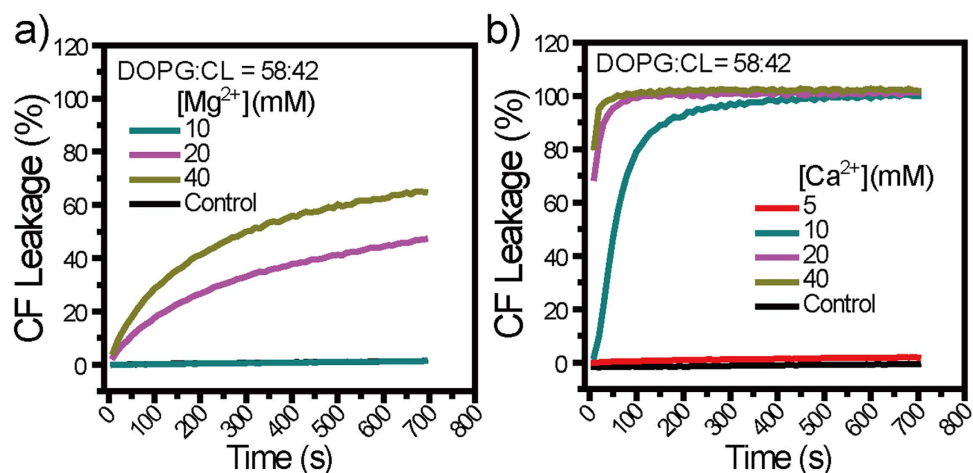


**Figure 2.** (a,b) Dye leakage assays using DOPG: CL = 58:42 LUVs as a more realistic model for *S. aureus* membranes. Obviously, both (a) Mg<sup>2+</sup> and (b) Ca<sup>2+</sup> caused significant CF leakage from DOPG: CL = 58:42 LUVs and, to do so, their minimum threshold concentrations are 20 and 10 mM, respectively. Controls are samples assayed similarly but without M<sup>2+</sup> addition.

appreciable CF leakage up to 40 mM (Fig. 1c), induced >30% lucigenin quenching (Fig. 1d) once  $\geq 20$  mM in similar assays but with CF being replaced with lucigenin—a membrane-impermeant, fluorescent Cl<sup>-</sup> indicator of similar molecular diameter as CF<sup>63-65</sup>, indicative of Ca<sup>2+</sup>-induced Cl<sup>-</sup> influx across membranes. Obviously, both Ca<sup>2+</sup> and Mg<sup>2+</sup> permeabilize CL membranes. That their distinct abilities to releases CF from CL LUVs correlate with the difference in water channel diameter of inverted hexagonal ( $H_{II}$ ) structures they induced in CL membranes (1.50 nm versus 2.42 nm)<sup>51</sup> further suggest that they may cause the observed membrane permeabilization by binding with CL to form negative-curvature M<sup>2+</sup>-CL complexes (M = Ca, Mg).

In addition to CL, phosphoglycerol (PG) is another major lipid component in *S. aureus* membranes<sup>49,50</sup>. To assess whether Ca<sup>2+</sup> and Mg<sup>2+</sup> permeabilize *S. aureus* membranes in which CL is diluted by PG, we use binary LUVs composed of DOPG:CL = 58:42 as a more realistic model for *S. aureus* membranes<sup>57</sup> and perform similar CF leakage assays as above. From DOPG:CL = 58:42 LUVs, Ca<sup>2+</sup> at  $\geq 10$  mM caused >90% CF leakage within 300 s after its addition, as compared to undetectable CF leakage caused by that at 5 mM (Fig. 2a), indicative of a minimum threshold Ca<sup>2+</sup> concentration of 10 mM. Similarly, Mg<sup>2+</sup> at  $\geq 20$  mM caused  $\geq 40\%$  CF leakage at 700 s after its addition, as compared to undetectable CF leakage by that at  $\leq 10$  mM (Fig. 2b), indicative of a minimum threshold Mg<sup>2+</sup> concentration of 20 mM. Obviously, both Ca<sup>2+</sup> and Mg<sup>2+</sup> permeabilize model *S. aureus* membranes despite that CL content is diluted by PG but, for them to do so, certain minimal threshold concentrations are required.

Both Ca<sup>2+</sup> and Mg<sup>2+</sup> are active against model *S. aureus* membranes. Does that necessarily correspond to antibacterial activity against *S. aureus* cells? To assess this, we evaluated the bactericidal activities of Ca<sup>2+</sup> and Mg<sup>2+</sup> by performing antibacterial plate killing assays. Note that bacterial cells in stationary phase are more resistant to environmental stresses and antibiotics than counterparts in logarithmic phase<sup>12,66,67</sup>. We hence used *S. aureus* cells in stationary phase, rather than those in logarithmic phase as normally do, for antibacterial assays. Our results (Fig. 3a) reveal that, after 40-min treatment with either Ca<sup>2+</sup> or Mg<sup>2+</sup>, *S. aureus* cells exhibit viability loss to varying extent in a dose-dependent manner, with a maximal viability loss of ~60% observed at M<sup>2+</sup> concentration of 40 mM, the highest dose tested. It is noteworthy that a relative loss of 60% in viability ratio corresponds to an absolute number density of  $\sim 3 \times 10^5$  CFU/mL (colony-forming units per milliliter) in bacterial cells killed. Taken together, these observations suggest that both Ca<sup>2+</sup> and Mg<sup>2+</sup> are definitively bactericidal against *S. aureus*.

Closer examinations on both membrane permeabilization experiments and antibacterial assays above suggest that Ca<sup>2+</sup> and Mg<sup>2+</sup> may be membrane-active against *S. aureus*. The minimal M<sup>2+</sup> dose required for killing

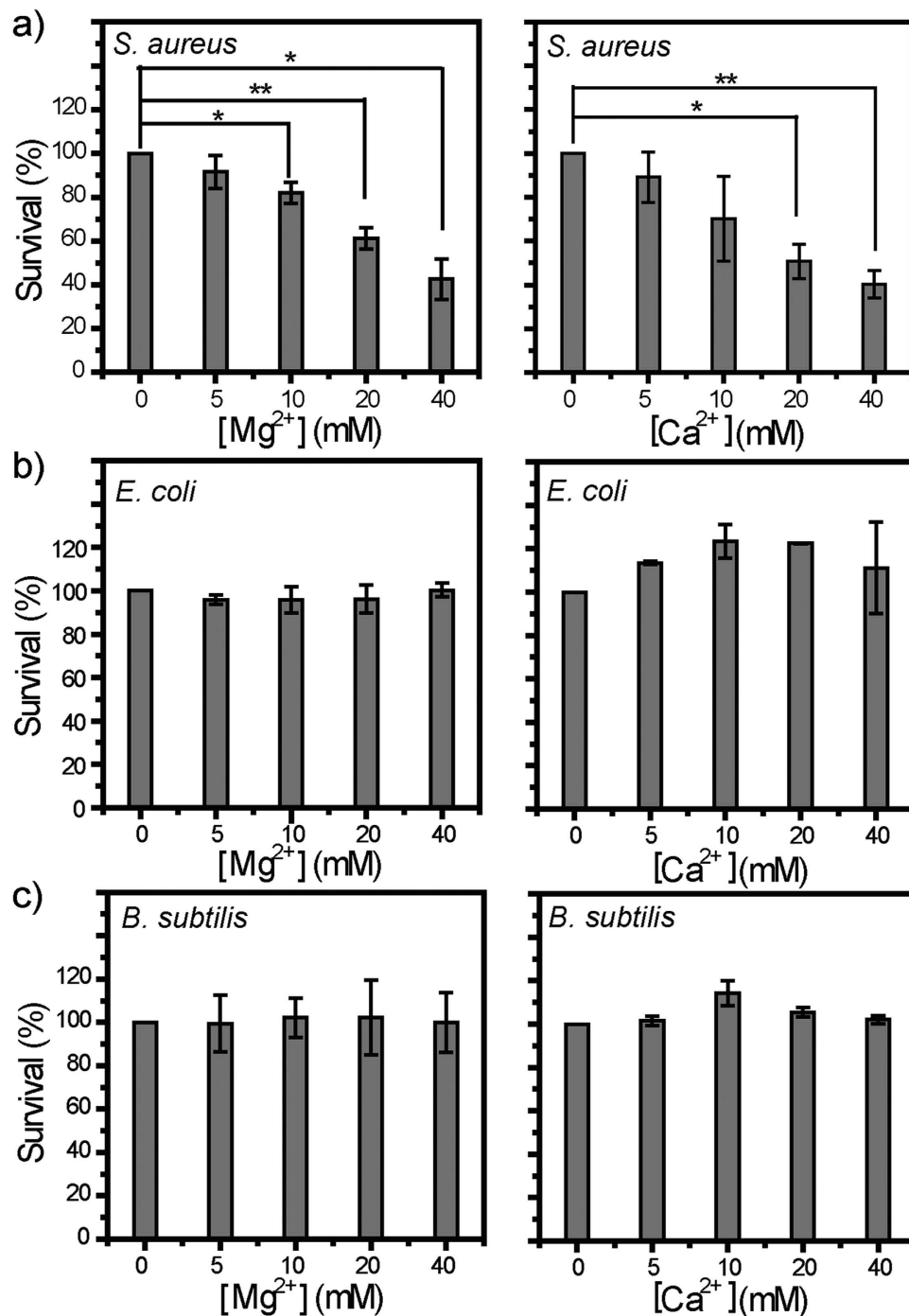


**Figure 3.** Plate killing assays against stationary-phase cells of (a) *S. aureus*, (b) *E. coli*, and (c) *B. subtilis*. After 40-min co-incubation with Mg<sup>2+</sup> (left) and Ca<sup>2+</sup> (right) at ≤40 mM, *S. aureus* cells exhibited dose-dependent loss in viability. In contrast, the viability of *E. coli* and *B. subtilis* cells is barely impacted in similar assays. Data points are reported as mean ± standard deviation. \*and\*\* indicate  $p < 0.05$  and  $p < 0.01$ , respectively.

significant ( $p < 0.05$ ) percentage of inoculated *S. aureus* cells are 10 and 20 mM for Ca<sup>2+</sup> and Mg<sup>2+</sup>, respectively (Fig. 3a), which correlate well with the respective minimal threshold M<sup>2+</sup> dose for these two cations to induce appreciable CF release from model *S. aureus* membranes (Fig. 2a,b), suggesting that Ca<sup>2+</sup> and Mg<sup>2+</sup> may kill *S. aureus* cells by disrupting their membranes.

In stark contrast to their definitive activity against *S. aureus*, Ca<sup>2+</sup> and Mg<sup>2+</sup> barely affect the viability of *E. coli* or *B. subtilis* (Fig. 3b,c), despite that *B. subtilis* is a Gram-positive bacterium as is *S. aureus*. Both *E. coli* and *B. subtilis* contain no/low CL in their membranes<sup>68</sup>. Thus, high CL content in *S. aureus* membrane may account for the observed activity of Ca<sup>2+</sup> and Mg<sup>2+</sup>.

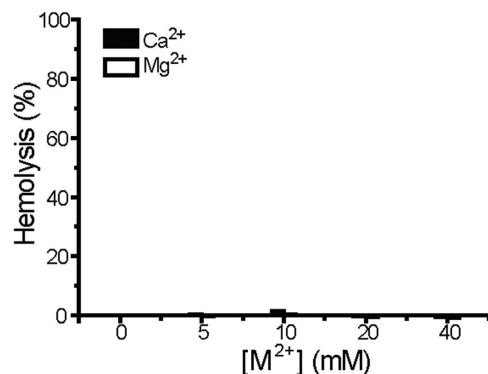


**Figure 4.** Up to 40 mM, neither Mg<sup>2+</sup> nor Ca<sup>2+</sup> caused detectable hemolysis against mouse red blood cells. Data points are reported as mean  $\pm$  standard deviation.

With species-specific antibacterial activity, MCl<sub>2</sub> solutions are distinct from their corresponding MO powder slurries, which are wide-spectrum disinfectants<sup>69–73</sup> used by human population of different cultures. Moreover, the observed activity of MCl<sub>2</sub> solutions suggests that M<sup>2+</sup> (M = Ca, Mg) ions may play contributive, rather than negligible, roles in the activity of their corresponding metal oxide (MO) powder slurries against *S. aureus*. To inhibit/kill  $\geq 50\%$  inoculated cells requires MO powder slurries of MO powder dose at a few mg/mL, which corresponds to 1–100 mM<sup>70,71,74,75</sup>. Frequently, M<sup>2+</sup> (M = Ca, Mg) ions produced *via* MO dissociation are viewed as negligible factors in the antibacterial activities of MO powder slurries<sup>74,76,77</sup>, due to inactivity of both the supernatant of MgO powder slurry and the MCl<sub>2</sub> solutions at concentrations 10-fold of the MO powder solubility values<sup>70,72</sup>. Note that M<sup>2+</sup> concentrations even 10-fold of MO powder solubility values are still  $< 10$  mM, which is within the barely-active dose range (Fig. 3a). Moreover, presence of *S. aureus* cells may actively retrieve free M<sup>2+</sup> to form M<sup>2+</sup>-CL complexes, a process which may promote MO dissociation and thus shift the effective M<sup>2+</sup> concentrations into the bactericidal range.

As potential antimicrobial agents, toxicity to host cells is a major concern. To preliminarily evaluate the toxicity of Mg<sup>2+</sup> and Ca<sup>2+</sup> ions, we performed hemolytic assays against mouse red blood cells. Within the tested concentration range (0–40 mM), neither Mg<sup>2+</sup> nor Ca<sup>2+</sup> caused  $> 5\%$  hemolysis (Fig. 4), indicative of good hemo-compatibility. Combined with the antibacterial assays (Fig. 3), these results suggest that Mg<sup>2+</sup> and Ca<sup>2+</sup> may preferentially eradicate *S. aureus* cells without affecting other bacteria or mammalian cells in the same niche.

## Conclusion

In summary, we found that Ca<sup>2+</sup> and Mg<sup>2+</sup> may be membrane-active, species-specific bactericidal agent against *S. aureus*. Moreover, within the tested concentration range, both Ca<sup>2+</sup> and Mg<sup>2+</sup> lack hemolytic toxicity. This work suggests that Ca<sup>2+</sup> and Mg<sup>2+</sup> may have implications in targeted eradication of *S. aureus* pathogen including antibiotic-resistant ones.

## Methods

**Materials.** *S. aureus* (ATCC 25923), *E. coli* (ATCC 25922) and *B. subtilis* (ATCC 6051) were purchased from American Type Culture Collection (ATCC) (Virginia, USA). Lipids used in this work, DOPG (1,2-dioleoyl-sn-glycero-3-[phospho-rac-(1-glycerol)] (sodium salt)), and TOCL (1,1',2,2'-Tetraoleoyl Cardiolipin, Sodium Salt) were purchased from Avanti Polar Lipids (Alabama, USA) and used without further purification. Carboxyl fluorescein (CF) was purchased from Sigma-Aldrich (Shanghai, China). Dehydrated Mueller-Hinton (MH) medium formulation and dehydrated Tryptic Soy Broth (TSB) medium formulation were purchased from Qingdao Hope Bio-Technology (Qingdao, China). All other reagents were purchased from Sinopharm Chemical Reagent Company (Shanghai, China). All reagents were used as supplied unless specified otherwise.

**Large Unilamellar Vesicle (LUV) Preparations.** LUVs composed of 100% CL and DOPG:CL = 58:42 were used as model cellular membranes for *S. aureus*<sup>57</sup> and prepared via extrusion. Into a glass vial, CL stock solution was added with or without stock solutions of DOPG; all lipid stock solutions were in chloroform at 20 mg/mL. The resulting lipid mixture was dried under gentle N<sub>2</sub> flow, desiccated in vacuum overnight, and rehydrated with CF (40 mM CF) or lucigenin (1 mM lucigenin, 50 mM NaNO<sub>3</sub>) solutions at 45 °C for 2 h. The resultant solution was subjected to five freeze-thaw cycles and subsequently extruded through a 0.4- $\mu$ m Nucleopore polycarbonate membrane (Whatman) for 21 times using a mini-extruder (Avanti Polar Lipids). External CF or lucigenin was removed by gel filtration (Sephadex G-25, GE healthcare) using HEPES buffer A (10 mM HEPES, 150 mM NaCl, pH = 7.4) as eluent.

**Characterizations on Membrane-Permeabilization.** Fluorescence emission intensity  $I_t$  for CF ( $\lambda_{ex} = 492$  nm,  $\lambda_{em} = 518$  nm) was monitored as a function of time ( $t$ ). Into a fluorimeter sample cuvette, we added expected CF-preloaded LUV suspension (900  $\mu$ L) and, at 200 s after initiation of  $I_t$  recording, M<sup>2+</sup>-containing HEPES solutions (1800  $\mu$ L in total, Table 1), to a final lipid concentration of 0.1 mM. At 900 s after initiation of  $I_t$  recording (*i.e.*, at 700 s after M<sup>2+</sup> addition), 50  $\mu$ L 10% triton was added, to yield  $I_\infty$  which indicates 100% CF leakage. The percentages of CF leakage were calculated as leakage (%) =  $(I_t - I_0)/(I_\infty - I_0) \times 100$ , where  $I_0$  is the

fluorescence intensity immediately (<10 s) after  $M^{2+}$  addition. Controls are samples assayed similarly but treated with  $M^{2+}$ -absent solution (i.e., 10 mM HEPES, 150 mM NaCl, pH 7.4).

**Antibacterial Assays.** The antibacterial activities of  $Ca^{2+}$  and  $Mg^{2+}$  were evaluated by performing classic plate killing assays against stationary-phase bacterial cells. For each bacterial strain, 3–5 individual bacterial colonies were inoculated into fresh sterile trypticase soy broth (TSB) and incubated at 37 °C with shaking (200 rpm) for 16 h to stationary phase. Bacterial cells were then harvested and washed twice with sterile HEPES buffer A (10 mM HEPES, 150 mM NaCl, pH 7.4) *via* centrifugation (2,500 rpm, Eppendorf 5810R) for 1 min and, within 15 min, adjusted with sterile HEPES buffer A (10 mM HEPES, 150 mM NaCl, pH 7.4) to  $\sim 1.5 \times 10^6$  CFU/mL and inoculated (50  $\mu$ L) into each zero-dilution well (150  $\mu$ L in total) of a preset 96-well microplate.

Expected amounts of divalent cation stock solutions (10 mM HEPES, 150 mM  $CaCl_2$  or  $MgCl_2$ , pH 7.4), sucrose stock solution (10 mM HEPES, 400 mM sucrose, pH 7.4), NaCl stock solution (10 mM HEPES, 500 mM NaCl, pH 7.4), and HEPES buffer B (10 mM HEPES, pH 7.4) were added into each zero-dilution well of a 96-well plate; all solutions were sterilized *via* filtering. After bacterial inoculation, final inoculum size in each zero-dilution well was  $\sim 5 \times 10^5$  CFU/mL and final buffer compositions in the zero-dilution wells are summarized in Table 1.

The microplate was then incubated at 37 °C with shaking (200 rpm) for 40 min. Serial 10-fold dilutions were subsequently made with sterile HEPES buffer A (10 mM HEPES, 150 mM NaCl, pH 7.4). Each dilution (20  $\mu$ L) was plated onto MH agar plates, which were then incubated at 37 °C overnight to give visible colonies. Inoculum size was indicated by control samples containing untreated bacteria. Each trial was performed in triplicate, and the reported results are the averages of two independent trials.

**Hemolysis assays.** Mouse blood was withdrawn from healthy mice obtained from the Animal Center of Anhui Medical University; the animal treatment was performed in compliance with the guidelines for the care and use of research animals established by the Animal Care and Use Committee at University of Science and Technology of China, and the experimental protocol was approved by the Animal Care and Use Committee at University of Science and Technology of China. Fresh mouse blood (200  $\mu$ L) was washed with sterile HEPES buffer (10 mM HEPES, 150 mM NaCl, pH = 7.4) (800  $\mu$ L) and washed for three times with sterile HEPES buffer *via* centrifuge at 900 rcf for 5 min, and the pellet was re-suspended into sterile HEPES buffer (1,000  $\mu$ L) to yield the mouse red blood cell (mRBC) stock suspension for hemolysis assays. The mRBC stock suspension (200  $\mu$ L) and  $MCl_2$ -containing HEPES solution (400  $\mu$ L) were added into each centrifuge cups. After the incubation at 37 °C for 40 min with shaking at 250 rpm, the centrifuge cups were centrifuged at 900 rcf for 5 min, and the supernatant (100  $\mu$ L) of each cup was transferred into a well of a 96-well microplate. Hemolysis was monitored by measuring the absorbance of the released hemoglobin at optical density at 414 nm,  $OD_{414}$ . Controls included HEPES buffer (300  $\mu$ L) and mRBC suspension (200  $\mu$ L) treated with triton X-100 (50%, 100  $\mu$ L) to provide reference for 0% and 100% hemolysis, respectively. Each hemolysis assay trial was carried out in triplicate, and the reported results are the averages of two independent trials.

**Statistical Analysis.** Statistical comparisons were carried out by performing student t test analysis with the statistical software package BioMedCalc (version 2.9). *p* values of <0.05 and <0.01 indicate statistical difference and statistically significant difference, respectively.

## References

- Chambers, H. F. & DeLeo, F. R. Waves of resistance: *Staphylococcus aureus* in the antibiotic era. *Nat. Rev. Microbiol.* **7**, 629–641, doi: 10.1038/nrmicro2200. (2009).
- Moore, C. E., Segal, S., Berendt, A. R., Hill, A. V. S. & Day, N. P. J. Lack of association between toll-like receptor 2 polymorphisms and susceptibility to severe disease caused by *Staphylococcus aureus*. *Clin. Diagn. Lab. Immunol.* **11**, 1194–1197, doi: 10.1128/Cdli.11.6.1194-1197.2004 (2004).
- Wertheim, H. F. L. & Verbrugh, H. A. Global prevalence of methicillin-resistant *Staphylococcus aureus*. *Lancet* **368**, 1866 (2006).
- Antibiotic Resistance Threats in the United States, 2013. Report by the U.S. Centers for Diseases Control and Prevention.
- Shai, Y. From Innate Immunity to de-Novo Designed Antimicrobial Peptides. *Curr. Pharm. Des.* **8**, 715–725, doi: 10.2174/1381612023395367 (2002).
- Yeaman, M. R. & Yount, N. Y. Mechanisms of Antimicrobial Peptide Action and Resistance. *Pharmacol. Rev.* **55**, 27–55 (2003).
- Wimley, W. C. Describing the Mechanism of Antimicrobial Peptide Action with the Interfacial Activity Model. *ACS Chem. Biol.* **5**, 905–917, doi: 10.1021/cb1001558 (2010).
- Hancock, R. E. W. & Sahl, H.-G. Antimicrobial and host-defense peptides as new anti-infective therapeutic strategies. *Nat. Biotechnol.* **24**, 1551–1557, doi: 10.1038/nbt1267 (2006).
- Brogden, K. A. Antimicrobial Peptides: Pore Formers or Metabolic Inhibitors in Bacteria? *Nat. Rev. Microbiol.* **3**, 238–250 (2005).
- Zaslouff, M. Antimicrobial Peptides of Multicellular Organisms *Nature* **415**, 389–395 (2002).
- Schmidt, N. W. *et al.* Criterion for Amino Acid Composition of Defensins and Antimicrobial Peptides Based on Geometry of Membrane Destabilization. *J. Am. Chem. Soc.* **133**, 6720–6727, doi: 10.1021/ja200079a (2011).
- Hurdle, J. G., O'Neill, A. J., Chopra, I. & Lee, R. E. Targeting bacterial membrane function: an underexploited mechanism for treating persistent infections. *Nat. Rev. Microbiol.* **9**, 62–75, doi: 10.1038/nrmicro2474 (2011).
- Oren, Z. & Shai, Y. Selective Lysis of Bacteria but Not Mammalian Cells by Diastereomers of Melittin: Structure-Function Study. *Biochemistry* **36**, 1826–1835 (1997).
- Chen, Y. *et al.* Rational Design of  $\alpha$ -Helical Antimicrobial Peptides with Enhanced Activities and Specificity/Therapeutic Index. *J. Biol. Chem.* **280**, 12316–12329 (2005).
- Won, H.-S., Jung, S.-J., Kim, H. E., Seo, M.-D. & Lee, B.-J. Systematic Peptide Engineering and Structural Characterization to Search for the Shortest Antimicrobial Peptide Analogue of Gaegurin 5. *J. Biol. Chem.* **279**, 14784–14791 (2004).
- Fernandez-Lopez, S. *et al.* Antibacterial agents based on the cyclic d,l-[ $\alpha$ ]-peptide architecture. *Nature* **412**, 452–455 (2001).
- Hamuro, Y., Schneider, J. P. & DeGrado, W. F. De Novo Design of Antibacterial  $\beta$ -Peptides. *J. Am. Chem. Soc.* **121**, 12200–12201 (1999).
- Porter, E. A., Wang, X., Lee, H.-S., Weisblum, B. & Gellman, S. H. Antibiotics: Non-haemolytic  $\beta$ -amino-acid Oligomers. *Nature* **404**, 565–565 (2000).

19. Liu, D. & DeGrado, W. F. De Novo Design, Synthesis, and Characterization of Antimicrobial beta-Peptides *J. Am. Chem. Soc.* **123**, 7553–7559 (2001).
20. Porter, E. A., Weisblum, B. & Gellman, S. H. Mimicry of Host-Defense Peptides by Unnatural Oligomers: Antimicrobial  $\beta$ -Peptides. *J. Am. Chem. Soc.* **124**, 7324–7330 (2002).
21. Hayouka, Z. *et al.* Interplay among Subunit Identity, Subunit Proportion, Chain Length, and Stereochemistry in the Activity Profile of Sequence-Random Peptide Mixtures. *J. Am. Chem. Soc.* **135**, 11748–11751, doi: 10.1021/ja406231b (2013).
22. Rapireddy, S. *et al.* RTD-1Mimic Containing  $\gamma$ PNA Scaffold Exhibits Broad-Spectrum Antibacterial Activities. *J. Am. Chem. Soc.* **134**, 4041–4044, doi: 10.1021/ja211867j (2012).
23. Patch, J. A. & Barron, A. E. Helical Peptoid Mimics of Magainin-2 Amide. *J. Am. Chem. Soc.* **125**, 12092–12093 (2003).
24. Tew, G. N. *et al.* De novo Design of Biomimetic Antimicrobial Polymers. *Proc. Natl. Acad. Sci. USA* **99**, 5110–5114 (2002).
25. Liu, D. *et al.* Nontoxic Membrane-Active Antimicrobial Arylamide Oligomers. *Angew. Chem. Int. Ed.* **43**, 1158–1162 (2004).
26. Tew, G. N., Clements, D., Tang, H., Arnt, L. & Scott, R. W. Antimicrobial activity of an abiotic host defense peptide mimic. *Biochim. Biophys. Acta, Biomembranes* **1758**, 1387–1392 (2006).
27. Choi, S. *et al.* De novo design and in vivo activity of conformationally restrained antimicrobial arylamide foldamers. *Proc. Natl. Acad. Sci. USA* **106**, 6968–6973, doi: 10.1073/pnas.0811818106 (2009).
28. Radziszewsky, I. S. *et al.* Improved antimicrobial peptides based on acyl-lysine oligomers. *Nat. Biotechnol.* **25**, 657–659, doi: 10.1038/nbt1309 (2007).
29. Thaker, H. D., Cankaya, A., Scott, R. W. & Tew, G. N. Role of Amphiphilicity in the Design of Synthetic Mimics of Antimicrobial Peptides with Gram-Negative Activity. *ACS Med. Chem. Lett.* **4**, 481–485, doi: 10.1021/ml300307b (2013).
30. Kuroda, K. & DeGrado, W. F. Amphiphilic Polymethacrylate Derivatives as Antimicrobial Agents. *J. Am. Chem. Soc.* **127**, 4128–4129 (2005).
31. Palermo, E. F., Sovadinova, I. & Kuroda, K. Structural Determinants of Antimicrobial Activity and Biocompatibility in Membrane-Disrupting Methacrylamide Random Copolymers. *Biomacromolecules* **10**, 3098–3107, doi: 10.1021/bm900784x (2009).
32. Lienkamp, K. *et al.* Antimicrobial Polymers Prepared by ROMP with Unprecedented Selectivity: A Molecular Construction Kit Approach. *J. Am. Chem. Soc.* **130**, 9836–9843, doi: 10.1021/ja801662y (2008).
33. Ilker, M. F., Nüsslein, K., Tew, G. N. & Coughlin, E. B. Tuning the Hemolytic and Antibacterial Activities of Amphiphilic Polynorbornene Derivatives. *J. Am. Chem. Soc.* **126**, 15870–15875 (2004).
34. Mowery, B. P. *et al.* Mimicry of Antimicrobial Host-Defense Peptides by Random Copolymers. *J. Am. Chem. Soc.* **129**, 15474–15476, doi: 10.1021/ja077288d (2007).
35. Sambhy, V., Peterson, B. R. & Sen, A. Antibacterial and Hemolytic Activities of Pyridinium Polymers as a Function of the Spatial Relationship between the Positive Charge and the Pendant Alkyl Tail. *Angew. Chem. Int. Ed.* **47**, 1250–1254, doi: 10.1002/anie.200702287 (2008).
36. Oda, Y., Kanaoka, S., Sato, T., Aoshima, S. & Kuroda, K. Block versus Random Amphiphilic Copolymers as Antibacterial Agents. *Biomacromolecules* **12**, 3581–3591, doi: 10.1021/bm200780r (2011).
37. Qiao, Y. *et al.* Highly dynamic biodegradable micelles capable of lysing Gram-positive and Gram-negative bacterial membrane. *Biomaterials* **33**, 1146–1153, doi: http://dx.doi.org/10.1016/j.biomaterials.2011.10.020 (2012).
38. Jiang, Y. *et al.* Acid-Activated Antimicrobial Random Copolymers: A Mechanism-Guided Design of Antimicrobial Peptide Mimics. *Macromolecules* **46**, 3959–3964, doi: 10.1021/ma400484b (2013).
39. Yang, L. *et al.* Synthetic Antimicrobial Oligomers Induce a Composition-Dependent Topological Transition in Membranes. *J. Am. Chem. Soc.* **129**, 12141–12147 (2007).
40. Yang, L. *et al.* Mechanism of a prototypical synthetic membrane-active antimicrobial: Efficient hole-punching via interaction with negative intrinsic curvature lipids. *Proc. Natl. Acad. Sci. USA* **105**, 20595–20600, doi: 10.1073/pnas.0806456105 (2008).
41. Som, A., Yang, L., Wong, G. C. L. & Tew, G. N. Divalent Metal Ion Triggered Membrane Activity in Cardiolipin Vesicles by Antimicrobial Molecule. *J. Am. Chem. Soc.* **131**, 15102–15103 (2009).
42. Hu, K. *et al.* A Critical Evaluation of Random Copolymer Mimesis of Homogeneous Antimicrobial Peptides. *Macromolecules* **46**, 1908–1915, doi: 10.1021/ma302577e (2013).
43. Perros, M. A sustainable model for antibiotics. *Science* **347**, 1062–1064, doi: 10.1126/science.aaa3048 (2015).
44. Borkow, G. & Gabbay, J. Copper as a biocidal tool. *Curr. Med. Chem.* **12**, 2163–2175, doi: 10.2174/0929867054637617 (2005).
45. Aghatabay, N. M. *et al.* Synthesis, characterization and antimicrobial activity of Fe(II), Zn(II), Cd(II) and Hg(II) complexes with 2,6-bis(benzimidazol-2-yl) pyridine ligand. *Eur. J. Med. Chem.* **42**, 205–213, doi: http://dx.doi.org/10.1016/j.ejmech.2006.09.023 (2007).
46. Chernousova, S. & Eppe, M. Silver as Antibacterial Agent: Ion, Nanoparticle, and Metal. *Angew. Chem. Int. Ed.* **52**, 1636–1653, doi: 10.1002/anie.201205923 (2013).
47. Jung, W. K. *et al.* Antibacterial Activity and Mechanism of Action of the Silver Ion in Staphylococcus aureus and Escherichia coli. *Appl. Environ. Microbiol.* **74**, 2171–2178, doi: 10.1128/aem.02001-07 (2008).
48. Cutinell, C. & Galdiero, F. Ion-Binding Properties of Cell Wall of Staphylococcus Aureus. *J. Bacteriol.* **93**, 2022–& (1967).
49. Short, S. A. & White, D. C. Metabolism of Phosphatidylglycerol, Lysylphosphatidylglycerol, and Cardiolipin of Staphylococcus aureus. *J. Bacteriol.* **108**, 219–226 (1971).
50. Tsai, M. *et al.* Staphylococcus aureus requires cardiolipin for survival under conditions of high salinity. *BMC Microbiol.* **11**, 13 (2011).
51. Rand, R. P. & Sengupta, S. Cardiolipin Forms Hexagonal Structures with Divalent Cations. *Biochim. Biophys. Acta, Biomembranes* **225**, 484–+ (1972).
52. Som, A. & Tew, G. N. Influence of Lipid Composition on Membrane Activity of Antimicrobial Phenylene Ethynylene Oligomers. *J. Phys. Chem. B* **112**, 3495–3502 (2008).
53. Wei, G. *et al.* Lipid Composition Influences the Membrane-Disrupting Activity of Antimicrobial Methacrylate Co-polymers. *J. Biomater. Sci. Polym. Ed.* **22**, 2041–2061, doi: 10.1163/092050610x530982 (2011).
54. Michael, R., Niesman, B. K. & Gholam, A. Peyman. Encapsulation of Sodium Fluorescein for Dye Release Studies. *Invest. Ophthalmol. Vis. Sci.* **33**, 2113–2119 (1992).
55. Chin, W. *et al.* Biodegradable Broad-Spectrum Antimicrobial Polycarbonates: Investigating the Role of Chemical Structure on Activity and Selectivity. *Macromolecules* **46**, 8797–8807, doi: 10.1021/ma4019685 (2013).
56. Ferdani, R. *et al.* Transport of chloride and carboxyfluorescein through phospholipid vesicle membranes by heptapeptide amphiphiles. *Org. Biomol. Chem.* **5**, 2423–2432, doi: 10.1039/b705544g (2007).
57. Epan, R. F. *et al.* Dual Mechanism of Bacterial Lethality for a Cationic Sequence-Random Copolymer that Mimics Host-Defense Antimicrobial Peptides. *J. Mol. Biol.* **379**, 38–50 (2008).
58. Mukherjee, S. *et al.* Antibacterial membrane attack by a pore-forming intestinal C-type lectin. *Nature* **505**, 103–107, doi: 10.1038/nature12729 (2014).
59. Yandek, L. E. *et al.* Mechanism of the cell-penetrating peptide transport 10 permeation of lipid bilayers. *Biophys. J.* **92**, 2434–2444, doi: 10.1529/biophysj.106.100198 (2007).
60. Delon, A., Usson, Y., Derouard, J., Biben, T. & Souchier, C. Continuous photobleaching in vesicles and living cells: a measure of diffusion and compartmentation. *Biophys. J.* **90**, 2548–2562, doi: 10.1529/biophysj.105.069815 (2006).

61. Patel, H., Tscheka, C. & Heerklotz, H. Characterizing vesicle leakage by fluorescence lifetime measurements. *Soft Matter* **5**, 2849, doi: 10.1039/b908524f (2009).
62. Breukink, E. *et al.* Lipid II Is an Intrinsic Component of the Pore Induced by Nisin in Bacterial Membranes. *J. Biol. Chem.* **278**, 19898–19903, doi: 10.1074/jbc.M301463200 (2003).
63. Richard Maskiewicz, D. S. & Thomas, C. Bruce. Chemiluminescent Reactions of Lucigenin. I. Reactions of Lucigenin with Hydrogen Peroxide. *J. Am. Chem. Soc.* **101**, 5347–5354 (1978).
64. Chen, Y. A Mechanism for Tamoxifen-mediated Inhibition of Acidification. *J. Biol. Chem.* **274**, 18364–18373, doi: 10.1074/jbc.274.26.18364 (1999).
65. William, A., Harrell, J., Marie Liesel Bergmeyer, Peter, Y. Zavalij & Jeffery, T. Davis. Ceramide-Mediated Transport of Chloride and Bicarbonate Across Phospholipid Membranes. *Chem. Commun.* **46**, 3950–3952 (2010).
66. Matin, A., Lynch, S. & Benoit, M. Increased bacterial resistance and virulence in simulated microgravity and its molecular basis. *Gravit. Space Res.* **19**, (2007).
67. Anderl, J. N., Zahller, J., Roe, F. & Stewart, P. S. Role of nutrient limitation and stationary-phase existence in *Klebsiella pneumoniae* biofilm resistance to ampicillin and ciprofloxacin. *Antimicrob. Agents Chemother.* **47**, 1251–1256, doi: 10.1128/Aac.47.4.1251-1256.2003 (2003).
68. Kamp, J. A. F. O. d., Redai, I. & Deenen, L. L. M. v. Phospholipid Composition of *Bacillus subtilis*. *J. Bacteriol.* **99**, 298–303 (1969).
69. Yamamoto, O., Ohira, T., Alvarez, K. & Fukuda, M. Antibacterial characteristics of CaCO<sub>3</sub>-MgO composites. *Mater. Sci. Eng. B Adv.* **173**, 208–212, doi: 10.1016/j.mseb.2009.12.007 (2010).
70. Sawai, J. Quantitative evaluation of antibacterial activities of metallic oxide powders (ZnO, MgO and CaO) by conductimetric assay. *J. Microbiol. Methods* **54**, 177–182, doi: 10.1016/S0167-7012(03)00037-X (2003).
71. Sawai, J., Himizu, K. & Yamamoto, O. Kinetics of bacterial death by heated dolomite powder slurry. *Soil Biol. Biochem.* **37**, 1484–1489, doi: 10.1016/j.soilbio.2005.01.011 (2005).
72. Sawai, J. *et al.* Antibacterial characteristics of magnesium oxide powder. *World J. Microbiol. Biotechnol.* **16**, 187–194, doi: 10.1023/A:1008916209784 (2000).
73. Sawai, J., Shiga, H. & Kojima, H. Kinetic analysis of the bactericidal action of heated scallop-shell powder. *Int. J. Food Microbiol.* **71**, 211–218, doi: 10.1016/S0168-1605(01)00619-5 (2001).
74. Sawai, J., Shiga, H. & Kojima, H. Kinetic analysis of death of bacteria in CaO powder slurry. *Int. Biodeter. Biodegr.* **47**, 23–26, doi: 10.1016/S0964-8305(00)00115-3 (2001).
75. Bae, D. H., Yeon, J. H., Park, S. Y., Lee, D. H. & Ha, S. D. Bactericidal effects of CaO (scallop-shell powder) on foodborne pathogenic bacteria. *Arch. Pharm. Res.* **29**, 298–301, doi: 10.1007/Bf02968574 (2006).
76. Siqueira, J. F. & Lopes, H. P. Mechanisms of antimicrobial activity of calcium hydroxide: a critical review. *Int. Endod. J.* **32**, 361–369, doi: 10.1046/j.1365-2591.1999.00275.x (1999).
77. Sawai, J. *et al.* Hydrogen peroxide as an antibacterial factor in zinc oxide powder slurry. *J. Ferment. Bioeng.* **86**, 521–522, doi: 10.1016/S0922-338x(98)80165-7 (1998).

## Acknowledgements

We thank Zhi Zhao and Kan Hu for assistance on fluorimeter experiments. This work was supported in part by the National Natural Science Foundation of China (Grants 11074178 and 21174138), the Youth Innovation Promotion Association of Chinese Academy of Sciences, and Anhui Education Department (KJ2013A267).

## Author Contributions

L.Y. conceived the idea, Y.X. conducted the research, and Y.X. and L.Y. analyzed the data and wrote the paper.

## Additional Information

**Competing financial interests:** The authors declare no competing financial interests.

**How to cite this article:** Xie, Y. and Yang, L. Calcium and Magnesium Ions Are Membrane-Active against Stationary-Phase *Staphylococcus aureus* with High Specificity. *Sci. Rep.* **6**, 20628; doi: 10.1038/srep20628 (2016).



This work is licensed under a Creative Commons Attribution 4.0 International License. The images or other third party material in this article are included in the article's Creative Commons license, unless indicated otherwise in the credit line; if the material is not included under the Creative Commons license, users will need to obtain permission from the license holder to reproduce the material. To view a copy of this license, visit <http://creativecommons.org/licenses/by/4.0/>